Systems & Control Transactions

Original Research Article
Peer Reviewed Conference Proceeding
ESCAPE 36 - European Symposium on Computer Aided Process Engineering
Sheffield, UK. 21-24 June 2026

PSE PRESS

Causal Discovery for the Spatial Autoregressive Model: Application to Defect Analysis in the Plastic Injection Molding Process

Ryosuke Tanaka[a][b], Koichi Fujiwara[a][c][d]*

[a] Nagoya University, Department of Materials Process Engineering, Nagoya, Aichi, Japan
[b] MCC Advanced Moldings Co., Ltd., Yokkaichi, Mie, Japan
[c] Hokkaido University, Research Institute for Electronic Science, Sapporo, Hokkaido, Japan
[d] Nara Institute of Science and Technology, Medilux Research Center, Ikoma, Nara, Japan
* Corresponding Author: fujiwara.koichi@hps.material.nagoya-u.ac.jp.

ABSTRACT

Plastic injection molding is a widely used polymer-processing method. As the requirements for processing accuracy have become increasingly stringent, defect analysis in plastic injection molding is necessary to improve the product yield. Causal discovery has recently gained attention for defect analysis in many processes. Because injection molding is a spatial process involving the distribution of physical quantities, spatial autocorrelation should be considered. Although the linear non-Gaussian acyclic model (LiNGAM) is a well-known causal discovery method, it cannot properly model spatial autocorrelation. In this study, a new causal discovery method for a spatially autocorrelated dependent variable, referred to as the Causal Structure Search for the Spatial Autoregressive Model (CASSPAR), is proposed. It models the causal relationships among the observed points without prior knowledge of the spatial structure. The proposed method represents the causal relationships among the observed points as a causal graph and estimates the adjacency matrix of the graph. The adjacency matrix is estimated using LiNGAM, and the model parameters are estimated using two-stage least squares (2SLS). The usefulness of the proposed CASSPAR was demonstrated using simulation data of a plastic injection molding process to identify the root cause of warpage.

Keywords: Polymers, Modelling and Simulations, Machine Learning, Algorithms

INTRODUCTION

Injection molding is a widely used polymer processing method in which a molten resin is injected into a mold and solidified to form a product. Warpage is a post-molding product deformation that hinders the manufacture of high-quality products. In Figure 1, warpage may occur in completely opposite directions depending on the process parameters, even for identical products, which makes it difficult to analyze and control the causes of defects. Warpage may be influenced by multiple factors, including the temperature distribution, pressure distribution, product geometry, and materials [1]. Because these mechanisms often vary across individual products, identifying the causes of warpage and modifying the process operations are crucial for improving product quality.

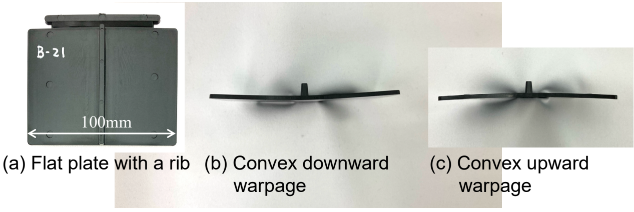

(a) Flat plate with a rib (b) Convex downward warpage (c) Convex upward warpage

Figure 1: An example of warpage. A product of the same shape exhibits warpage in opposite directions depending on process parameters

Simulation studies have been successfully applied to predict warpage and optimize the process operations. Chen *et al.* investigated process variables affecting warpage using a design of experiments (DOE) on simulation data [2]. In addition, the response surface method (RSM) in multi-objective optimization for warpage suppression and cycle time has been reported [3].

Machine learning (ML) techniques have also been applied to defect analysis. For instance, a warpage prediction model was constructed using random forests [4], and neural networks (NN) were trained on time-series data of in-mold pressure [5].

However, ML models and ML model-based optimization often become black boxes. Although they may achieve good performance in warpage prediction, their lack of interpretability makes it challenging to identify the root causes of warpage and develop fundamental countermeasures.

Causal discovery has gained attention for analyzing industrial process data [6, 7]. The linear non-Gaussian acyclic model (LiNGAM) is a well-known causal discovery method that estimates the causal structure among variables as a graph [8]. A key feature of LiNGAM is its statistical identifiability; it can uniquely identify the causal graph from observational data alone without prior knowledge. Various LiNGAM extensions have been proposed, including time-series data [9]. However, existing variants do not take spatial information into account.

Injection molding is considered a spatial process because physical quantities, such as temperature and pressure, are distributed across the product and mold. For example, spatial nonuniformity in temperature and stress can induce warpage [10, 11].

Spatial autocorrelation needs to be considered in spatial data, which means that observations at neighboring points are mutually dependent. This characteristic violates the independence assumption underlying many statistical methods, such as linear regression [12]. LiNGAM estimates also become biased from spatial data because each variable is no longer independent due to spatial autocorrelation. Therefore, a new causal discovery method for addressing spatial autocorrelation is required.

To express the relationship among observed points, a spatial weight matrix $\mathbf{W} \in \mathbb{R}^{N \times N}$ is used, where $\mathbf{W}$ can be defined as the adjacency or distance matrix between two points, and N is the number of points. The spatial autoregressive (SAR) model is a widely used regression method that uses $\mathbf{W}$ to incorporate the dependent variable y at neighboring locations as a predictor.

In most spatial models, $\mathbf{W}$ has to be given in advance, which means that the spatial autocorrelation is already known; however, this assumption is unrealistic for injection molding processes because it is difficult to observe such a relationship during molding. To estimate the spatial weight matrix $\mathbf{W}$ without prior constraints becomes difficult when the number of elements in $\mathbf{W}$ exceeds the number of observed points N. Thus, the structure of $\mathbf{W}$ has to be constrained with some assumptions [13]. However, it is unclear whether the injection molding process data satisfy these assumptions.

A key idea of this study is to interpret $\mathbf{W}$ as a representation of causal relationships because the spatial distributions in the injection molding process always follow the causal relationship by physicochemical mechanisms. Thus, $\mathbf{W}$ is regarded as an adjacency matrix of a causal graph. By applying LiNGAM, $\mathbf{W}$ can be uniquely identified and estimated directly from the data.

This study proposes a new causal discovery method for the spatial autoregressive model, referred to as the Causal Structure Search for the Spatial Autoregressive Model (CASSPAR). The proposed CASSPAR reveals causal relationships among locations without prior knowledge of spatial structure. This capability enables more precise defect analysis of warpage, leading to improved product yield and reduced energy consumption and costs. The estimation performance of CASSPAR is demonstrated through its application to simulation data of an injection-molding process.

METHOD

The proposed CASSPAR interprets the spatial weight matrix $\mathbf{W}$ in the SAR model as a spatial causal structure and estimates $\mathbf{W}$ using LiNGAM. The background on LiNGAM and the SAR model is provided, and the estimation procedure of CASSPAR is explained in the following sections.

Linear non-Gaussian acyclic model (LiNGAM)

LiNGAM is a causal discovery method that represents causal relationships among variables using a directed acyclic graph. Figure 2 shows an example of a causal graph used to investigate the causes of warpage in injection molding. The strength of the causal relationship is denoted by a coefficient b. In LiNGAM, each observed variable x_i is expressed as a linear sum of other observed variables x_j and an error term e_i. The causal graph in Figure 2 corresponds to the following structural equations:

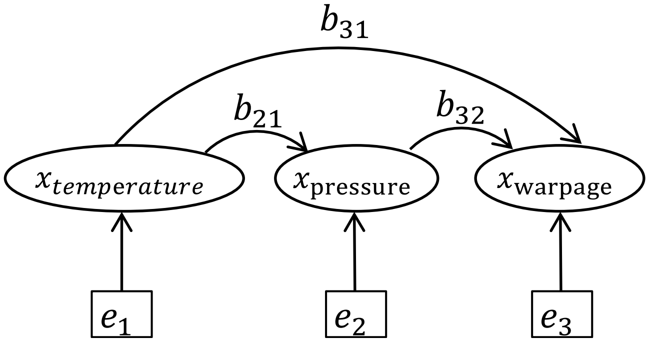

Figure 2: An example of a causal structure estimated by LiNGAM, represented as a causal graph.

$$\begin{aligned} x_{temperature} &= e_1 \\ x_{pressure} &= b_{21}x_{temperature} + e_2 \\ x_{warpage} &= b_{31}x_{temperature} + b_{32}x_{pressure} + e_3. \end{aligned} \quad (1)$$

This figure illustrates the causal relationships, indicating that warpage is affected by both the process temperature and pressure, and that pressure is also affected by the temperature. In matrix form, Eq. (1) is written as

$$\mathbf{x} = \mathbf{B}\mathbf{x} + \mathbf{e} \quad (2)$$

where $\mathbf{B} \in \mathbb{R}^{K \times K}$ denotes the adjacency matrix of the causal graph to be estimated, $\mathbf{x} \in \mathbb{R}^{K}$ is the vector of K observed variables, and $\mathbf{e} \in \mathbb{R}^{K}$ represents the vector of error terms. To ensure the identifiability of the causal graph, the following assumptions are required: 1) The error variables follow non-Gaussian distributions and are mutually independent. 2) The causal graph is acyclic, which means that no directed cycles exist in the causal graph.

Spatial autoregressive (SAR) model

Spatial autocorrelation is a key characteristic of spatial data, which is the tendency for observations at neighboring locations to be more similar (or dissimilar) than those at more distant locations. Positive spatial autocorrelation corresponds to a pattern in which neighboring locations have similar values.

The spatial weight matrix $\mathbf{W} \in \mathbb{R}^{N \times N}$ is used to model spatial autocorrelation, which is a matrix representation of the adjacency relationships among N locations. Figure 3 shows typical definitions of $\mathbf{W}$. The element w_{ij} in $\mathbf{W}$ represents the influence of location j on location i. The diagonal elements w_{ii} are set to zero to avoid influencing itself. For reasons of computational stability and interpretability, $\mathbf{W}$ is commonly row-standardized so that each row sums to one. Figure 3 (a)–(c) show an example of a typical $\mathbf{W}$ indicating which locations affect the central cell shown in red. Color intensity represents the strength of the influence.

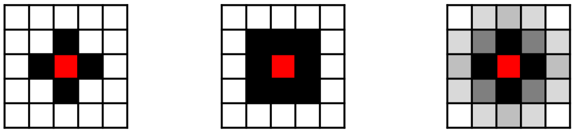

(a) Rook adjacency (b) Queen adjacency (c) Distance based W

Figure 3. Typical definitions of the spatial weight matrix $\mathbf{W}$ in 3 × 3 lattice space.

Various spatial regression models can be defined depending on which variable, dependent variable, independent variable, or error term exhibits spatial autocorrelation. This study focuses on the spatial autoregressive (SAR) model, also called the spatial lag model (SLM), which assumes that the dependent variable y is spatially autocorrelated. This assumption is natural for warpage prediction, and the dependent variable y represents warpage. Warpage exhibits positive spatial autocorrelation because deformation at one location typically causes the surrounding areas to deform in the same direction. The SAR model is given by

$$y_i = \rho \sum_{j=1}^{N} w_{ij}\, y_j + \mathbf{X_i}\beta + e_i \quad (3)$$

where y_i is the dependent variable at location i, ρ denotes the spatial autocorrelation coefficient, w_{ij} represents the spatial weight between locations i and $j, \mathbf{X_i} \in \mathbb{R}^{K}$ is a vector of K independent variables at location $i, \boldsymbol{\beta} \in \mathbb{R}^{K}$ is a coefficient vector, and e_i is the error term at location i.

Figure 4 presents a schematic of the SAR model used to predict warpage in injection molding. As shown, the dependent variable y_i, which represents warpage, is influenced by neighboring warpages, such as y_j, y_k, y_l. In addition, y_i is influenced by other variables $\mathbf{X_i}$ at the same location (e.g., product temperature and pressure), as well as by the error term e_i.

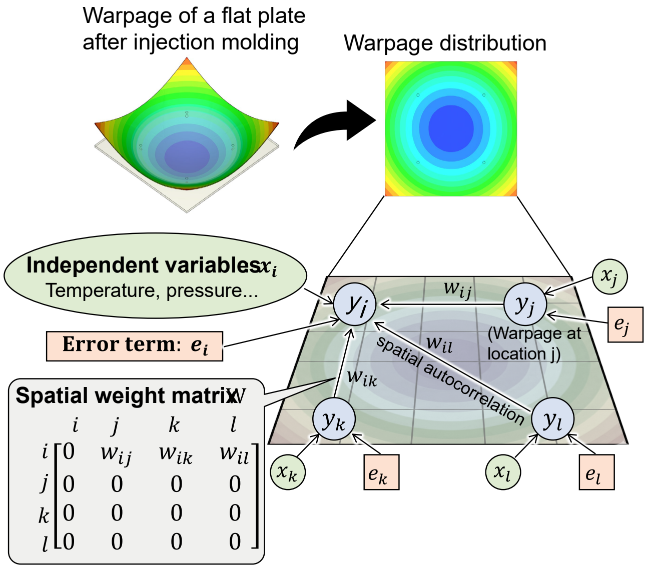

Figure 4: A schematic of SAR model for predicting warpage in injection molding.

The spatial autocorrelation coefficient ρ denotes the strength of the influence that a location receives from its neighbors. A large positive value of ρ represents a positive spatial autocorrelation. The term $\sum_{j=1}^{N} w_{ij}\, y_j$ is called the spatial lag. The variables ρ and $\boldsymbol{\beta}$ are the model parameters to estimate.

Causal Structure Search for the Spatial Autoregressive Model (CASSPAR).

CASSPAR estimates the spatial weight matrix $\mathbf{W}$ and the SAR parameters: $\rho, \boldsymbol{\beta}$. To apply LiNGAM to spatial data, the SAR model is reformulated. The matrix form of the SAR model is defined as

$$\mathbf{Y} = \rho \mathbf{W}\mathbf{Y} + \mathbf{X}\boldsymbol{\beta} + \mathbf{e} \tag{4}$$

where $\mathbf{Y} \in \mathbb{R}^{T \times N}$ and $\mathbf{X} \in \mathbb{R}^{T \times N \times K}$ denote the measurements of the dependent and independent variables, respectively. $\mathbf{W} \in \mathbb{R}^{N \times N}$ is a spatial weight matrix, ρ and $\boldsymbol{\beta} \in \mathbb{R}^{K}$ are spatial autoregressive coefficient and regression coefficient vectors, and $\mathbf{e}$ is an error term. Note that $\mathbf{W}$ is assumed to be row-standardized and spectrally normalized.

Algorithm 1 Step 1: Estimation of spatial weight matrix $\hat{\mathbf{W}}$

```
1. Input:
   Observed dependent variable matrix $\mathbf{Y} \in \mathbb{R}^{T \times N}$
2. Output:
   Estimated spatial weight matrix after normalization $\hat{\mathbf{W}} \in \mathbb{R}^{N \times N}$
3. Apply the Direct-LiNGAM algorithm to $\mathbf{Y}$ and obtain an estimated adjacency matrix $\hat{\mathbf{A}} \in \mathbb{R}^{N \times N}$.
4. $\hat{\mathbf{A}}$ is first row-standardized and then spectrally normalized to obtain the normalized matrix $\hat{\mathbf{W}}$.
5. Return $\hat{\mathbf{W}}$
```

By defining $\mathbf{A} = \rho \mathbf{W}$ and $\mathbf{e}' = \mathbf{X}\boldsymbol{\beta} + \mathbf{e}$, SAR can be reformulated in the same form as the LiNGAM model:

$$\mathbf{Y} = \mathbf{A}\mathbf{Y} + \mathbf{e}' \tag{5}$$

This reformulation allows us to estimate the spatial structure using LiNGAM. However, the following assumptions are required for LiNGAM identification:

Assumption 1: Spatial weight matrix $\mathbf{W}$ (and thus $\mathbf{A}$) corresponds to an adjacency matrix of a directed acyclic graph (DAG). In other words, $\mathbf{A}$ can be permuted into a strictly lower triangular matrix. This assumption is natural in the context of injection molding, where the resin flows in one direction, that is, the influence propagates only from upstream to downstream locations.

Assumption 2: Each component of the external error vector $\boldsymbol{e}'$ follow a non-Gaussian distribution, and they are mutually independent.

This study proposes a two-step estimation procedure. In step 1, the structure of the spatial weight matrix $\mathbf{W}$ is estimated, and in step 2, the SAR parameters ρ and $\boldsymbol{\beta}$ are estimated. Figure 5 illustrates the procedure of the proposed CASSPAR.

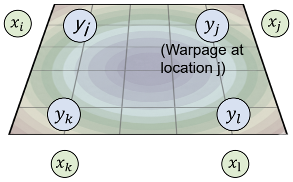

(a) Observed variables in lattice space

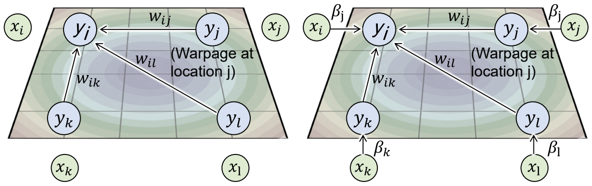

(b) Step1: Estimation of causal structure

(c) Step2: Estimation of coefficients

Figure 5: Conceptual illustration of the proposed two-step estimation procedure.

Step 1: Estimation of the spatial weight matrix

The Direct-LiNGAM algorithm [14] is applied to the reformulated LiNGAM model in Eq. (5), and the estimated adjacency matrix $\hat{\mathbf{A}} \in \mathbb{R}^{N \times N}$ is obtained. Although step 1 estimates the adjacency matrix $\hat{\mathbf{A}}$, a normalized weight matrix $\mathbf{W}$ is required for step 2. Therefore, $\hat{\mathbf{W}}$ is obtained by row-standardizing and spectral normalizing $\hat{\mathbf{A}}$ (Algorithm 1).

Step 2: Estimation of SAR Parameters via 2SLS

Given $\hat{\mathbf{W}}$, the SAR parameters ρ and $\boldsymbol{\beta}$ are estimated by an instrumental variables (IV) approach based on two-stage least squares (2SLS). Using the normalized spatial weight matrix $\hat{\mathbf{W}}$ obtained in Step 1, the original SAR equation is formulated as:

$$\mathbf{Y} = \rho \hat{\mathbf{W}}\mathbf{Y} + \mathbf{X}\boldsymbol{\beta} + \mathbf{e}. \tag{6}$$

The endogenous problem arises in Eq. (6) because the spatial lag term $\hat{\mathbf{W}}\mathbf{Y}$ is simultaneously determined with dependent variable $\mathbf{Y}$. Consequently, $\hat{\mathbf{W}}\mathbf{Y}$ is correlated with the error term $\mathbf{e}$. Due to this endogeneity, OLS estimates biased ρ and $\boldsymbol{\beta}$. Thus, this study adopts the IV method to estimate these parameters, which is a standard estimation method for SAR models [15].

For the convenience of the IV method, Eq. (6) is rearranged as follows: let $\mathbf{y}_t \in \mathbb{R}^{N}$ and $\mathbf{X}_t \in \mathbb{R}^{N \times K}$ denote the t-th sample of $\mathbf{Y}$ and $\mathbf{X}$, respectively, $\mathbf{y}_{\text{stack}} \in \mathbb{R}^{TN}$ and $\mathbf{X}_{\text{stack}} \in \mathbb{R}^{TN \times K}$ are vertically stacked matrices of $\{\mathbf{y}_t\}_{t=1}^{T}$ and $\{\mathbf{X}_t\}_{t=1}^{T}$. The corresponding stacked spatial lag term is defined as

$$\mathbf{S} = [(\hat{\mathbf{W}}\mathbf{y}_1)^{\top}, \ldots, (\hat{\mathbf{W}}\mathbf{y}_T)^{\top}]^{\top} \in \mathbb{R}^{TN}. \tag{7}$$

Using $\mathbf{S}$, the SAR model can be expressed as

$$\mathbf{y}_{\text{stack}} = \rho \mathbf{S} + \mathbf{X}_{\text{stack}}\boldsymbol{\beta} + \mathbf{e}_{\text{stack}} \tag{8}$$

where $\mathbf{e}_{\text{stack}} \in \mathbb{R}^{TN}$ denotes the stacked error term.

The instrument variable $\mathbf{Z}$ is constructed from the exogenous variables $\mathbf{X}$ and their spatial lags. For each lag order $\ell = 1, \dots, L$, the matrices

$$\mathbf{Z}_t^{(\ell)} = \widehat{\mathbf{W}}^{\ell}\mathbf{X}_t \in \mathbb{R}^{N \times K} \tag{9}$$

are defined, and $\mathbf{Z}^{(\ell)} \in \mathbb{R}^{TN \times K}$ is obtained by stacking $\{\mathbf{Z}_t^{(\ell)}\}_{t=1}^{T}$ vertically. The full instrument matrix is then given by

$$\mathbf{Z} = [\mathbf{X}_{\text{stack}}, \mathbf{Z}^{(1)}, \dots, \mathbf{Z}^{(L)}] \in \mathbb{R}^{TN \times K(L+1)}. \tag{10}$$

This IV procedure requires the following assumptions about the instruments:

Assumption 3: The exogenous variables are uncorrelated with the error term $e, \mathrm{Cov}[Z, e] = 0$, to ensure that the instruments are exogenous and valid for the two-stage least squares (2SLS) estimation.

Assumption 4: The instruments are correlated with the endogenous spatial lag term $S, \mathrm{Cov}[Z, S] \neq 0$, which means that the instruments have sufficient relevance for the spatial lag term.

The SAR parameters ρ and β can be estimated via the 2SLS method. In the first stage of 2SLS, the endogenous spatial lag term $\mathbf{S}$ is regressed on the instrument matrix $\mathbf{Z}$ by OLS, and the fitted values $\hat{\mathbf{S}}$ are obtained. In the second stage, $\mathbf{y}_{\text{stack}}$ is regressed on $[\hat{\mathbf{S}}, \mathbf{X}_{\text{stack}}]$ by OLS. The coefficient on $\hat{\mathbf{S}}$ and the coefficient vector on $\mathbf{X}_{\text{stack}}$ yield the 2SLS estimates $\hat{\rho}$ and $\hat{\boldsymbol{\beta}}$, respectively. Under Assumptions 1-4, these estimators are consistent with the parameters of the original SAR. Algorithm 2 describes the procedure of SAR parameter estimation.

Algorithm 2 Step 2: Estimation of SAR parameters ρ and β via 2SLS

```
1. Input:
     Normalized spatial weight matrix $\widehat{\mathbf{W}} \in \mathbb{R}^{N \times N}$.
     Observed dependent variable matrix $\mathbf{Y} \in \mathbb{R}^{T \times N}$.
     Observed independent variables tensor $\mathbf{X} \in \mathbb{R}^{T \times N \times K}$.
2. Output:
     Spatial autoregressive coefficient $\hat{\rho} \in \mathbb{R}$.
     Regression coefficients $\hat{\boldsymbol{\beta}} \in \mathbb{R}^{K}$.
3. Stack $\mathbf{Y}$ and $\mathbf{X}$ over samples to obtain $\mathbf{y}_{\text{stack}} \in \mathbb{R}^{TN}$ and $\mathbf{X}_{\text{stack}} \in \mathbb{R}^{TN \times K}$.
4. Consider the SAR model with the estimated spatial weight, $\mathbf{y}_{\text{stack}} = \rho\mathbf{S} + \mathbf{X}_{\text{stack}}\boldsymbol{\beta} + \mathbf{e}_{\text{stack}}$ here, $\mathbf{S}$ is the stacked spatial lag term.
5. Construct the instrument matrix for the $t$-th sample: $\mathbf{Z}_t = \left[\mathbf{X}_t,\ \widehat{\mathbf{W}}\mathbf{X}_t,\ \widehat{\mathbf{W}}^2\mathbf{X}_t,\ \dots,\ \widehat{\mathbf{W}}^L\mathbf{X}_t\right] \in \mathbb{R}^{TN \times K(L+1)}$
6. Apply two-stage least squares (2SLS) to the stacked SAR with the spatially lagged term as the endogenous regressor and $\mathbf{Z}$ as the instrument matrix, Obtain the estimates $\hat{\rho}$ and $\hat{\boldsymbol{\beta}}$.
7. Return $\hat{\rho}, \hat{\boldsymbol{\beta}}$
```

APPLICATION TO SIMULATION OF INJECTION MOLDING

In this section, the application results of the proposed CASSPAR to simulation data of injection molding to verify its capability to identify the causes of warpage are reported.

One of the primary causes of warpage is a non-uniform temperature distribution. Figure 6 (a) shows the 3D model of the injection-molding process used in the simulation, and (b)-(d) illustrate the mechanism of product deformation: (b) a temperature difference exists between the top and bottom of the product, which (c) leads to non-uniform resin shrinkage during solidification, and (d) consequently causes product deformation.

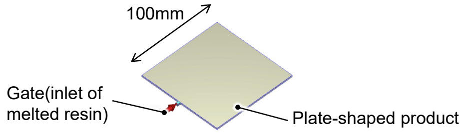

(a) 3D model of the injection molding process used for the simulation.

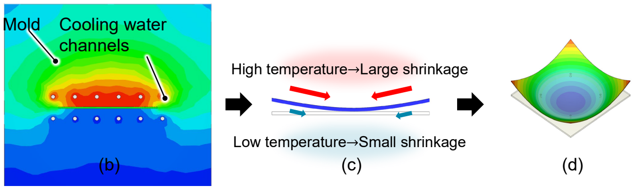

Figure 6: (a) 3D model of the injection molding process used for the simulation; (b)-(d) show the mechanisms of warpage.

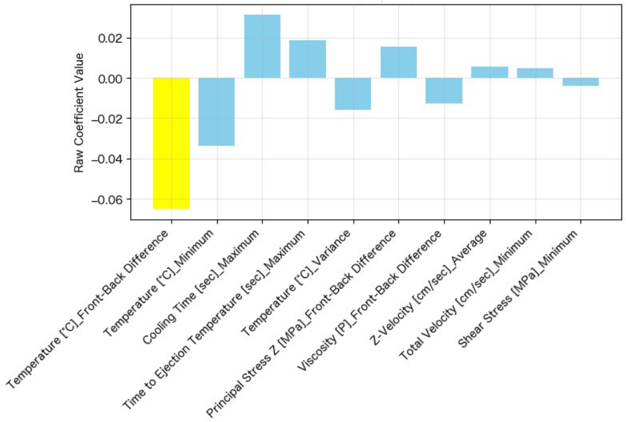

Figure 7: The top 10 largest absolute coefficient values estimated by the proposed CASSPAR.

In the simulation, a temperature difference between the top and bottom surfaces was intentionally introduced. A 9×9 grid of measurement points $(N = 81)$ was placed on the plate for data collection. The data included variables such as the warpage, temperature difference between the top and bottom of the product, pressure, and resin flow velocity. The warpage at the 81 locations was treated as the endogenous spatial variable Y, whereas the temperature difference, pressure, and flow velocity were treated as the exogenous variables X.

Figure 7 shows the top 10 largest absolute coefficient values estimated by the proposed CASSPAR. The top-ranked variable, "Temperature [℃]_Front-Back Difference, " represents the temperature difference between the top and bottom surfaces of the product. This result indicates that the proposed CASSPAR successfully identified the intentionally introduced temperature difference as the top-ranking causal factor of warpage.

Figure 8 shows the estimated spatial weight matrix W for the warpage, which is expected to exhibit positive spatial autocorrelation because a deformation at one location typically induces deformations in the same direction in the surrounding areas. The estimated $\mathbf{W}$ exhibits a local neighborhood structure similar to contiguity-based matrices, such as rook or queen adjacency.

This result suggests that the proposed CASSPAR successfully captured the physically reasonable spatial interactions underlying the warpage deformation.

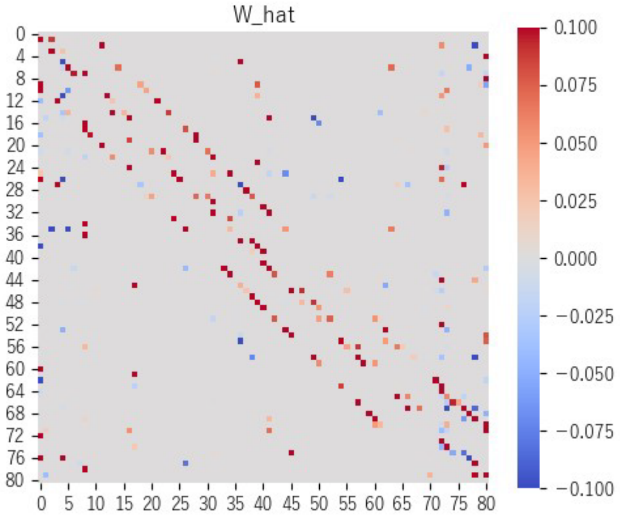

Figure 8. Heatmap of the estimated spatial weight matrix $\mathbf{W}$.

CONCLUSIONS

In this study, a new causal discovery method for spatial data, referred to as CASSPAR, was proposed. A limitation of this study is that CASSPAR considers spatial autocorrelation only in the dependent variable Y. However, in many industrial processes, the independent variables X may also exhibit spatial dependence. CASSPAR can also be applicable to other spatially dependent processes, such as fault diagnosis in chemical plants and semiconductor wafer manufacturing. Future work includes validation in real-world experiments and extension to industrial processes beyond injection molding.

ACKNOWLEDGEMENTS

This work was based on the results obtained from project JPNP20004, subsidized by the New Energy and Industrial Technology Development Organization (NEDO).

REFERENCES

1. Coca-Gonzalez M, Jimenez-Martinez M. Warpage: causes, manufacturing processes and future challenges: a review. Proceedings of the Institution of Mechanical Engineers, Part L: Journal of Materials: Design and Applications 239:1201-1217 (2024). https://doi.org/10.1177/14644207241285399
2. Chen CP, Chuang MT, Hsiao YH, Yang YK, Tsai CH. Simulation and experimental study in determining injection molding process parameters for thin-shell plastic parts via design of experiments analysis. Expert Systems with Applications 36:10752-10759 (2009). https://doi.org/10.1016/j.eswa.2009.02.017
3. Kitayama S, Yokoyama M, Takano M, Aiba S. Multi-objective optimization of variable packing pressure profile and process parameters in plastic injection molding for minimizing warpage and cycle time. Int J Adv Manuf Technol 92:3991-3999 (2017). https://doi.org/10.1007/s00170-017-0456-1
4. Ahmed, T., Sharma, P. & Karmaker, C. Warpage prediction of Injection-molded PVC part using ensemble machine learning algorithm. Mater. Today Proc. 50, (2020).
5. Gim J, Lin CY, Turng LS. In-mold condition-centered and explainable artificial intelligence-based (IMC-XAI) process optimization for injection molding. Journal of Manufacturing Systems 72:196-213 (2024). https://doi.org/10.1016/j.jmsy.2023.11.013
6. Uchida Y, Fujiwara K, Saito T, Osaka T. Causal plot: causal-based fault diagnosis method based on causal analysis. Processes 10:2269 (2022). https://doi.org/10.3390/pr10112269
7. Xue J, Zhang T, Ye H. Kpi-oriented process monitoring based on causal-weighted partial least squares. Information Sciences 689:121470 (2025). https://doi.org/10.1016/j.ins.2024.121470
8. Shimizu, S., Hoyer, P. O. & Hyvärinen, A. A Linear Non-Gaussian Acyclic Model for Causal Discovery. Journal of Machine Learning Research vol. 7 (2006).
9. Hyvärinen, A., Zhang, K., Shimizu, S. & Hoyer, P. O. Estimation of a Structural Vector Autoregression Model Using Non-Gaussianity. J. Mach. Learn. Res. 11, 1709–1731 (2010).
10. Wang J, Liu T, Zheng K, Liu H, Cui H, Li H. Local

thermal warpage deformation of polypropylene injection molded flat part and neural network prediction model. Front. Mater. 11: (2024). https://doi.org/10.3389/fmats.2024.1421546

11. Choi S, Im YT. Prediction of shrinkage and warpage in consideration of residual stress in integrated simulation of injection molding. Composite Structures 47:655-665 (1999). https://doi.org/10.1016/s0263-8223(00)00045-3
12. Pace R, LeSage J. Spatial econometrics. Chapman & Hall/CRC Handbooks of Modern Statistical Methods :245-260 (2010). https://doi.org/10.1201/9781420072884-c15
13. Ahrens A, Bhattacharjee A. Two-step lasso estimation of the spatial weights matrix. Econometrics 3:128-155 (2015). https://doi.org/10.3390/econometrics3010128
14. Shimizu, S. et al. DirectLiNGAM: A Direct Method for Learning a Linear Non-Gaussian Structural Equation Model. The Journal of Machine Learning Research 12, 1225–1248 (2011).
15. Kelejian HH, Prucha IR. A generalized spatial two-stage least squares procedure for estimating a spatial autoregressive model with autoregressive disturbances. The Journal of Real Estate Finance and Economics 17:99-121 (1998). https://doi.org/10.1023/a:1007707430416
